iScience

Article

Fine-tuning of Wnt signaling by RNA surveillance factor Smg5 in the mouse craniofacial development

Graphical abstract

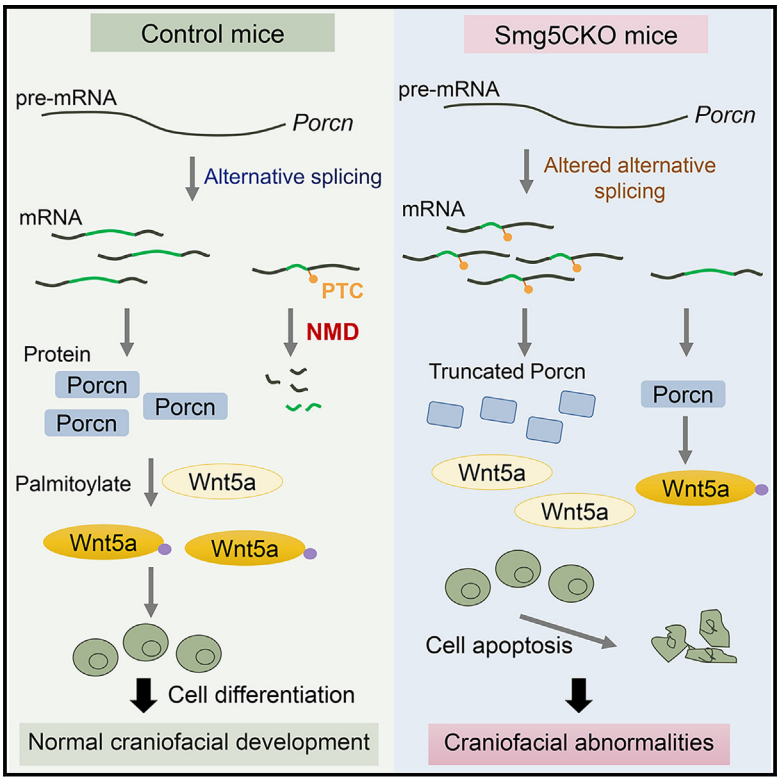

Highlights

- *Smg5* knockout in mice causes craniofacial defects, including cleft palate
- *Smg5* loss induces apoptosis and disrupts differentiation in craniofacial region
- *Smg5* deficiency increases PTC-containing mRNA and alters alternative splicing
- *Porcn* is identified as a key target regulated by Smg5-mediated NMD

Authors

Shicheng Zhu, Suman Huo, Weiran He, ..., Mengsheng Qiu, Tangliang Li, Xiao-Jing Zhu

Correspondence

li.tangliang@sdu.edu.cn (T.L.), xiao_jingzhu@hznu.edu.cn (X.-J.Z.)

In brief

Pathophysiology; Cell biology; Developmental biology

Zhu et al., 2025, iScience *28*, 111972
March 21, 2025
https://doi.org/10.1016/j.isci.2025.111972

CellPress

iScience

CellPress
OPEN ACCESS

Article

Fine-tuning of Wnt signaling by RNA surveillance factor Smg5 in the mouse craniofacial development

Shicheng Zhu,[1,5] Suman Huo,[1,5] Weiran He,[1] Caiyan Huang,[1] Jiannan Zhang,[1] Xiaoning Jiang,[2] Yeqing Qian,[3] Chengyan Chen,[4] Zhong-Min Dai,[1] Xueqin Yang,[1] Mengsheng Qiu,[1] Tangliang Li,[2,4,*] and Xiao-Jing Zhu[1,6,*]

[1]College of Life and Environmental Sciences, Zhejiang Key Laboratory of Organ Development and Regeneration, Hangzhou Normal University, Hangzhou, Zhejiang 311121, China
[2]School of Basic Medical Sciences, Hangzhou Normal University, Hangzhou, Zhejiang 311121, China
[3]Women's Hospital, Zhejiang University School of Medicine, Hangzhou, Zhejiang 310006, China
[4]State Key Laboratory of Microbial Technology, Shandong University, Qingdao 250100, China
[5]These authors contributed equally
[6]Lead contact
*Correspondence: li.tangliang@sdu.edu.cn (T.L.), xiao_jingzhu@hznu.edu.cn (X.-J.Z.)
https://doi.org/10.1016/j.isci.2025.111972

SUMMARY

The specific roles of nonsense-mediated mRNA decay (NMD), a translation-dependent RNA quality control mechanism that degrades mRNAs containing premature termination codons (PTCs), in mammalian craniofacial development have remained unclear. Here, we show that knockout of the essential NMD factor *Smg5* in mouse craniofacial neural crest cells leads to hypoplastic mandibles, subsequently inducing tongue mispositioning and cleft palate formation. Furthermore, *Smg5* loss triggers massive cell apoptosis and disrupts cell differentiation, accompanied by widespread alterations in alternative splicing and a surge in PTC-containing mRNA levels. Notably, the abnormal upregulation of a PTC-containing *Porcn* transcript leads to reduced Porcn protein and impaired Wnt5a/JNK signaling, a crucial pathway for craniofacial morphogenesis. Finally, death of Smg5-deficient craniofacial neural crest cells can be ameliorated by Wnt5a in craniofacial neural crest (CNC) *in vitro* explants. Taken together, our findings demonstrate that *Smg5*-mediated NMD regulates mammalian craniofacial development by fine-tuning Wnt signaling through post-transcriptional regulation of *Porcn*.

INTRODUCTION

Cleft palate represents one of the most common craniofacial birth defects in humans.[1] Craniofacial neural crest cells (CNCCs) play a central role in orofacial development. CNCCs originate from the dorsal aspect of the neural tube, migrate to facial primordia, proliferate and differentiate to mesenchymal cells, and give rise to a wide variety of craniofacial structures: most of the skeletal element, cartilage, nerve, and connective tissues.[2,3] During embryonic development, palatal shelves of the secondary palate arise from the medial projections of the facial maxillary processes, grow vertically along the lateral sides of the tongue, elevate to horizontal direction above the tongue, and fuse at the midline. Cleft palate can be caused by improper growth or fusion problem of the palatal shelves.[4] Additionally, inappropriate positioning of the tongue and reduced growth of Meckel's cartilage also results in cleft palate.[5,6]

The development of a cleft palate is correlated with genetic or environmental factors or their combination in craniofacial development. Altered Wnt signaling activity is highly associated with cleft palate.[7] For example, *Wnt5a* is expressed in the CNCCs-derived mesenchyme and mice lacking Wnt5a or its receptor Ror2 exhibit shortened mandible and cleft palate with a failure in palatal shelf elevation.[8] *Wnt1-Cre*-mediated deletion of *Wntless*, which is essential for Wnt trafficking, in mouse craniofacial mesenchyme inhibits Wnt5a-mediated noncanonical WNT signaling and leads to cleft palate.[9] Additionally, mesenchymal deficiency of *Porcn*, encoding the porcupine O-acyltransferase required for lipid modification of WNTs, also results in cleft palate.[10] However, how the WNT signaling activity is tightly controlled by post-transcriptional mechanisms during craniofacial development remains elusive.

Nonsense-mediated mRNA decay (NMD) is a translation-dependent RNA surveillance machinery that recognizes and eliminates mRNAs containing premature termination codons (PTCs) to maintain cellular RNA homeostasis.[11] An estimated one-third of the alternative transcripts in the human transcriptome contain PTCs, making alternative splicing coupled to NMD to be an efficient means to regulate gene expression.[12] In addition to its quality-control function, NMD targets around 10% of normal gene transcripts in response to cellular needs.[13] Through modulating mRNA stability, NMD actively participates in cell fate transition between stem cells and their somatic progenies.[11,14–16] There are two main routes for mRNA degradation in NMD: SMG5/7-dependent and SMG6-dependent decay of target mRNAs. Functional dependency is found between these

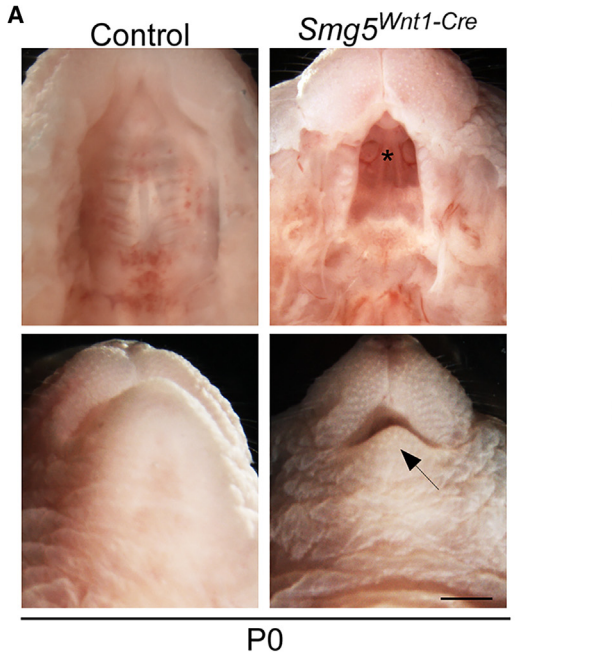

Figure 1. *Smg5* is required for secondary palate development in mice

(A) The $Smg5^{Wnt1\text{-}Cre}$ mice display a wide-open cleft secondary palate (asterisk) and a small mandible (indicated by an arrow).

(B) Comparison of the length and width of mandible in control and $Smg5^{Wnt1\text{-}Cre}$ embryos at P0 ($n = 3$). Data are shown as mean ± SEM. Student's t test, $^*p < 0.05$. Scale bars: 1 mm in (A) and 400 μm in (B).

two pathways: the loss of SMG5/7-dependent NMD could inactivate the SMG6-dependent branch, and the presence of either SMG5 or SMG7 is sufficient to support SMG6-mediated endonucleolysis of NMD targets.[17] Intriguingly, SMG5 can substitute the role of SMG7 and individually activate NMD.[17]

Previous studies have shown that NMD factors are required for early embryogenesis, as knockout of NMD genes including *Upf1*, *Upf2*, *Smg1*, and *Smg6* cause early embryonic lethality.[15,18–21] Mechanistically, NMD destabilizes mRNAs with various NMD features, such as long 3′ UTRs and PTCs, to safeguard the proper differentiation of embryonic stem cells.[15,16] In addition, NMD plays a critical role in development and homeostasis of tissue-specific stem cells. For example, knocking out *Smg6* in neural stem cells starting from mouse embryonic stage E10.5 causes mild neurogenesis defects in the cortex.[22] Hematopoietic stem cell-specific deletion of *Upf2* results in the extinction of all hematopoietic stem and progenitor populations.[20] *Upf2* also plays crucial roles in the development of prospermatogonia in neonatal mice, as well as during the first wave of spermatogenesis in puberty mice.[23] Mutations in *SMG9* lead to a multiple congenital anomaly syndrome in humans and mice.[24]

In this study, we investigate the function of NMD in regulating mouse craniofacial development using mouse model with *Smg5* specifically deleted in mouse CNCCs-derived mesenchyme. We show that *Smg5* is required for craniofacial development in mice. *Smg5* null mesenchyme shows delayed cell differentiation and aberrant cell apoptosis. Additionally, loss of *Smg5* in developing mesenchyme leads to altered alternative splicing events and accumulation of PTC-containing mRNA isoforms in developing mandibles. Moreover, our findings demonstrate an essential role for *Smg5*-mediated NMD in mammalian craniofacial development through post-transcriptional control of *Porcn* to regulate the Wnt signaling pathway.

RESULTS

Smg5 loss causes cleft palate in mice

To investigate the role of *Smg5*-mediated NMD in craniofacial development, we crossed *Smg5* conditional knockout mouse line with the *Wnt1-Cre* line to inactivate *Smg5* in CNCCs-derived mesenchyme (Figure S1). $Smg5^{Wnt1\text{-}Cre}$ mice displayed evident craniofacial abnormalities in especially small mandible and a complete cleft secondary palate with 100% penetrance (Figures 1A and 1B). *Smg5* knockout mice died after birth, primarily attributed to the inability to suckle effectively due to cleft palate. Histological analysis showed that $Smg5^{Wnt1\text{-}Cre}$ palatal shelves were deformed from E12.5 (Figures 2A and 2B). At E14.5, the palatal shelves of control mice have elevated to the horizontal position, met in the midline, and initiated fusion (Figure 2C). By contrast, the palatal shelves of $Smg5^{Wnt1\text{-}Cre}$ failed to grow horizontally and remained at the vertical position, resulting in a clefting defect (Figure 2C). It is noteworthy that $Smg5^{Wnt1\text{-}Cre}$ exhibited a mispositioned tongue (Figures 1B and 2C), which may obstruct the elevation of the palatal shelves and contribute to the cleft palate. Additionally, the elevation of one side of the palatal shelves occurred at later stages in $Smg5^{Wnt1\text{-}Cre}$ embryos (Figure 2D), suggesting that the palatal shelves depleted of *Smg5* still possess intrinsic competency for elevation. Additionally, we performed *in vitro* palate fusion assay to determine whether palatal fusion was affected due to loss of Smg5. The results showed that palatal shelves lacking Smg5 reserve the ability to fuse (Figure S2). Using $Smg5^{Wnt1\text{-}Cre}$ mice and their littermates carrying a $ROSA^{mT/mG}$ allele, we also found CNCCs of $Smg5^{Wnt1\text{-}Cre}$ migrated to the facial primordia as in their control littermates (Figure S3), suggesting that Smg5 deficiency did not disturb the normal migration of CNCCs. Taken together, these results suggest that the primary reason for the cleft palate may be attributed to micrognathia and the resulting obstruction caused by the tongue.

Deficiency of Smg5 leads to massive cell apoptosis in CNCCs-Derived mesenchyme

To identify the cellular defects underlying abnormal secondary palate development in $Smg5^{Wnt1\text{-}Cre}$, we performed TUNEL assay to examine cell apoptosis in the developing palatal shelves at E13.5. The results revealed massive cell apoptosis all over the

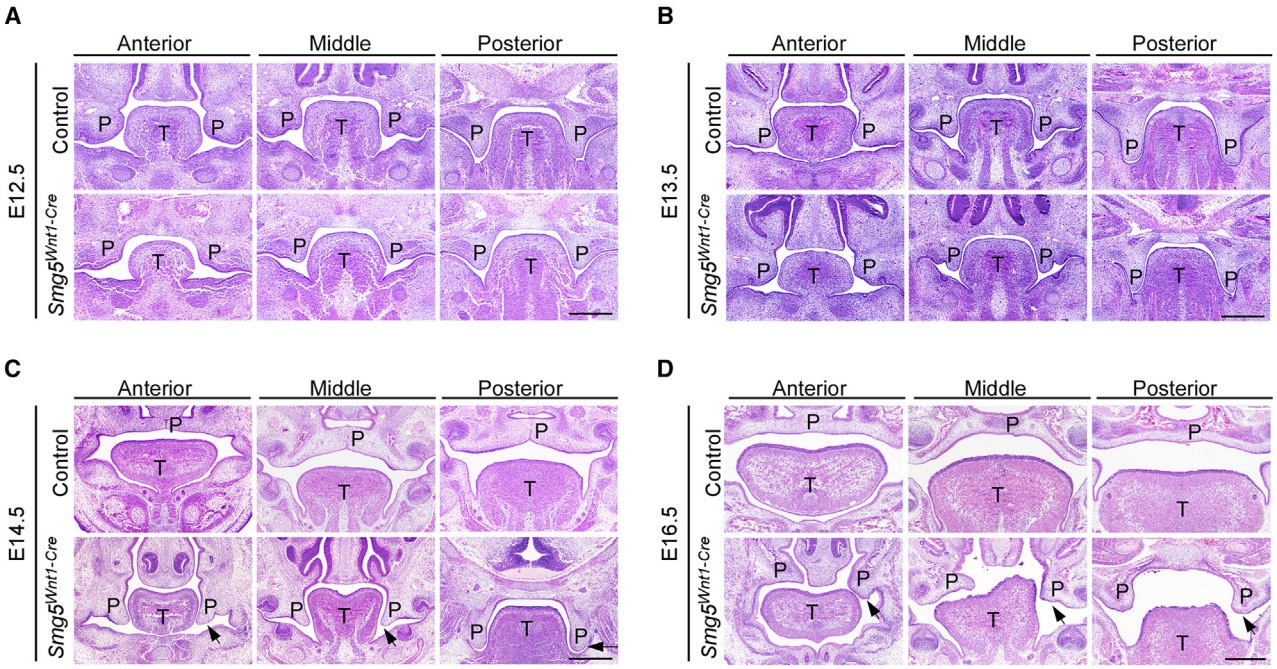

Figure 2. Histological analyses of frontal sections of control and *Smg5*$^{Wnt1\text{-}Cre}$ embryos at various developmental stages

(A–D) Embryonic heads from wild-type and *Smg5*-deficient mice were collected, fixed by 4% PFA, paraffin-embedded, sectioned into 7-μm slices, and stained with hematoxylin and eosin. The palatal shelves of *Smg5*$^{Wnt1\text{-}Cre}$ embryos exhibit evident abnormal shapes at E12.5 and E13.5 (A, B) and fail to elevate and become cleft at E14.5 (C). Elevation of one side of the palatal shelves occurred in *Smg5*$^{Wnt1\text{-}Cre}$ at E16.5 (D), suggesting that the Smg5-deficient palatal shelves still reserve the potential to elevate. Arrows indicate the failure of palatal elevation in *Smg5*$^{Wnt1\text{-}Cre}$ mice. P, palate; T, tongue. Scale bars, 400 μm.

craniofacial mesenchyme, including palatal shelves and the mandible (Figures 3A–3C). To further investigate the effect of *Smg5* deficiency on CNCCs, we performed *in vitro* culture of CNC explants from *Smg5*$^{Wnt1\text{-}Cre}$ mice and their littermates, both of which were carrying a *ROSA*$^{mT/mG}$ allele as a Cre reporter. In response to Cre recombination, CNCCs and their derivatives expressing Cre have cell membrane-localized EGFP (mG) fluorescence expression instead of tdTomato in mouse carrying a *ROSA*$^{mT/mG}$ allele. As revealed by EGFP fluorescence, the CNCCs migrated normally from both control and *Smg5*$^{Wnt1\text{-}Cre}$ CNC explants (Figures 3D–3K). Consistent with the *in vivo* results, a great reduction in green fluorescence was observed in *Smg5*$^{Wnt1\text{-}Cre}$ explants from day 4 of culture (Figures 3I–3K). The fluorescence intensity of *Smg5*$^{Wnt1\text{-}Cre}$ gradually decreases during *in vitro* culture, with control explants showing approximately twice the fluorescence intensity of *Smg5*$^{Wnt1\text{-}Cre}$ from day 4 (Figure 3L). These results suggest that cell apoptosis occurs in CNCCs that migrated from *Smg5*$^{Wnt1\text{-}Cre}$ CNC explants. Taken together, these results suggest that *Smg5* is required for the survival of CNCCs during craniofacial development.

Chondrogenesis of Meckel's cartilage and intramembranous ossification of mandible bone are impaired in Smg5$^{Wnt1\text{-}Cre}$

Given the link between cleft palate and small mandible,[5] our findings of micrognathia in *Smg5* knockout mice prompted us to investigate the timing and mechanisms of mandibular development disruption caused by Smg5 deficiency, confirming that the cleft palate is a consequence of the small mandible. Histological analysis revealed that the mesenchymal condensation of Meckel's cartilage was delayed in *Smg5*$^{Wnt1\text{-}Cre}$ mice. At E11.5, mesenchymal cells aggregated in the presumptive Meckel's cartilage region in the control mice but were absent in *Smg5*$^{Wnt1\text{-}Cre}$ mice (Figure 4A). As the development proceeded, the Meckel's cartilage was formed in *Smg5*$^{Wnt1\text{-}Cre}$ mice but was finer than in the control mice (Figure 4A). Next, we examined the expression of *Col2a1* and Sox9, the characteristic markers of chondrocytes, by *in situ* hybridization and immunofluorescent analysis in control and *Smg5*$^{Wnt1\text{-}Cre}$ mice. Both *Col2a1* and Sox9 expression were greatly decreased in *Smg5*$^{Wnt1\text{-}Cre}$ (Figure 4B). Western blot analysis also revealed a dramatically decreased Sox9 level in mandibles lacking Smg5 (Figure 4D), suggesting that the chondrogenic differentiation was disturbed in *Smg5*$^{Wnt1\text{-}Cre}$ mice. Consistent with the above results, *Smg5*$^{Wnt1\text{-}Cre}$ mice exhibited a marked reduction in Meckel's cartilage size from E13.5 (Figure 4C). These results revealed that the small mandible appeared before the elevation of the palatal shelves at E14.5, indicating that the cleft palate in *Smg5*$^{Wnt1\text{-}Cre}$ mice could be largely attributed to the small mandible.

As a transient structure, Meckel's cartilage disappears as the development proceeds.[25] It is noteworthy that the Meckel's cartilage of *Smg5*$^{Wnt1\text{-}Cre}$ does not disappear as in its littermates at E18.5 (Figure 4C), suggesting that the molecular program controlling this disappearance process is disrupted in response to Smg5 deficiency. Furthermore, the ossification of the mandible

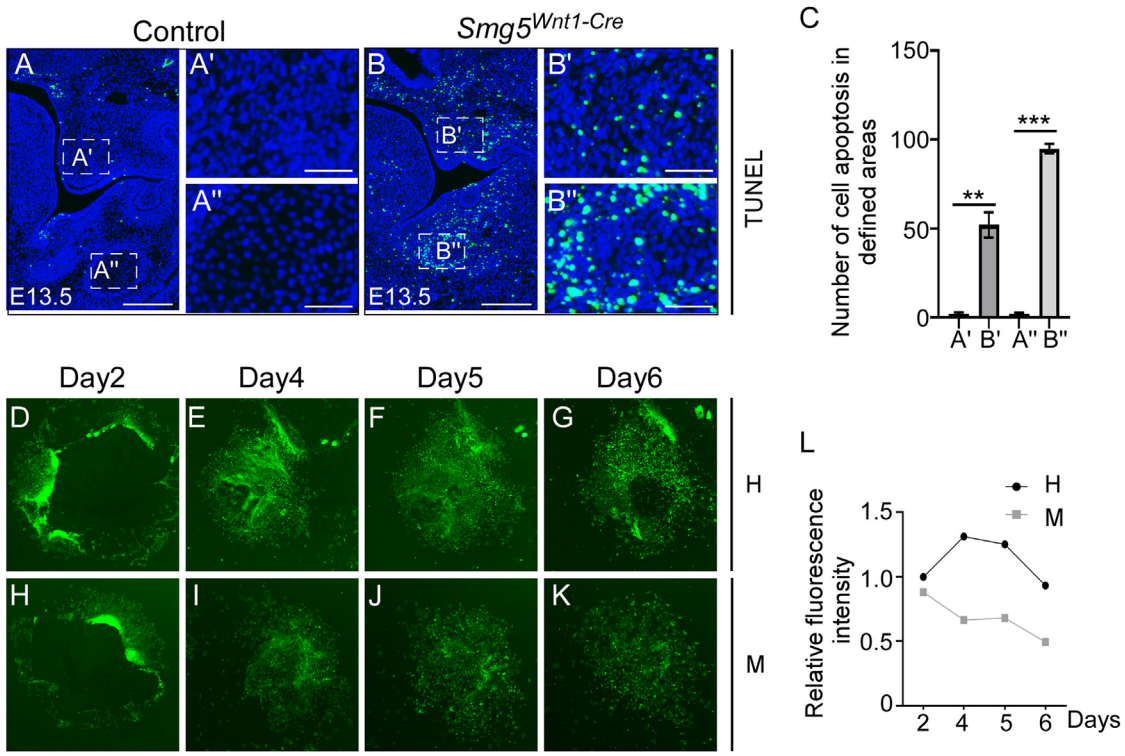

Figure 3. Aberrant cell death in *Smg5*-deficient CNCCs-derived craniofacial mesenchyme and CNC explants

(A and B) TUNEL staining analysis shows that loss of *Smg5* induces dramatic ectopic cell apoptosis all over the mesenchyme of the developing maxillary and mandible (n = 3). A′, B′, A″, B″. Magnified pictures of A and B.

(C) Number of apoptotic cells in designated areas of the palatal shelves (A′, B′) and the mandible (A″, B″). Data are shown as mean ± SEM. Student's t test, $^{**}p < 0.01$; $^{***}p < 0.001$.

(D–K) *In vitro* organ culture experiments show greatly decreased EGFP fluorescence in CNCCs that migrated from *Smg5*$^{f/+}$;*ROSA*$^{mT/mG}$;*Wnt1-Cre* (H) and *Smg5*$^{f/f}$;*ROSA*$^{mT/mG}$;*Wnt1-Cre* (M) CNC explants in a 6-day culture (n = 3).

(L) Representative relative fluorescence intensity in control (H) and *Smg5*-deficient mice (M) in D–K, normalized to day 2 control. Scale bars: 200 μm in (A) and (B) and 50 μm in others.

bone was delayed in *Smg5*$^{Wnt1\text{-}Cre}$ mice. Intramembranous ossification was observed in control but not *Smg5*$^{Wnt1\text{-}Cre}$ mandible bone at E15.5 (Figure 4C), followed by a greatly reduced bone size in *Smg5*-deficient mandibles at E18.5 (Figure 4C). The expression levels of Runx2 and Sp7, two transcription factors critical for osteoblast differentiation,[26–28] were severely decreased in the developing mandible at E13.5 (Figure 4D), which may account for the impaired mandible bone formation in *Smg5*$^{Wnt1\text{-}Cre}$ mice. In sum, these results suggest that *Smg5* depletion compromises cell differentiation in developing mouse mandibles.

Defective NMD activity in Smg5$^{Wnt1-Cre}$ mice

To examine whether NMD function is affected by *Smg5*-deficiency, we analyzed the expression of general NMD targets in control and *Smg5*-deficient mandibles at E13.5. We first analyzed the alternative splicing-coupled NMD by RT-PCR analysis. In the absence of Smg5, the level of the PTC-containing NMD target transcripts with features of both exon inclusion (*Hnrnpl, Jmjd6, Srsf2, Tmem183a, Rpl3*) and exon exclusion (*Hnrnph1, Hnrnph3, Mgea5, Ptbp2, Trub2*) was greatly increased (Figures 5A and 5B). The percent spliced-in values also indicate significant alterations in the splicing of these genes. Additionally, the expression of several NMD target transcripts, including *Atf4*, *Ddit3*, *Gas5*, and *1810032O08Rik,* was significantly upregulated in *Smg5*$^{Wnt1\text{-}Cre}$ mandibles (Figure 5C). Collectively, these results suggest that *Smg5* is essential for NMD in CNCCs-derived mesenchyme during embryonic development.

Smg5 deficiency leads to altered alternative splicing events in developing mouse craniofacial tissue

Next, we investigated the intrinsic molecular mechanism by which *Smg5*-mediated NMD may regulate craniofacial development. RNA sequencing (RNA-seq) analysis at multiple developmental stages revealed that *Smg5* deficiency significantly affected gene expression and the alternative splicing events in developing mandibles (Figure 6A; Tables S1, S2, S3, and S4). As NMD can affect the outcome of alternative splicing, we used differentially expressed transcripts (DETs) instead of differentially expressed genes for analysis. Increasing number of DETs was found in *Smg5*$^{Wnt1\text{-}Cre}$ mandibles at E10.5, E11.5, and E13.5 (Figure 6B). It is noteworthy that, for each stage, the number of increased DETs in *Smg5*$^{Wnt1\text{-}Cre}$ is at least 3-fold of that of downregulated DETs, which is probably caused by the

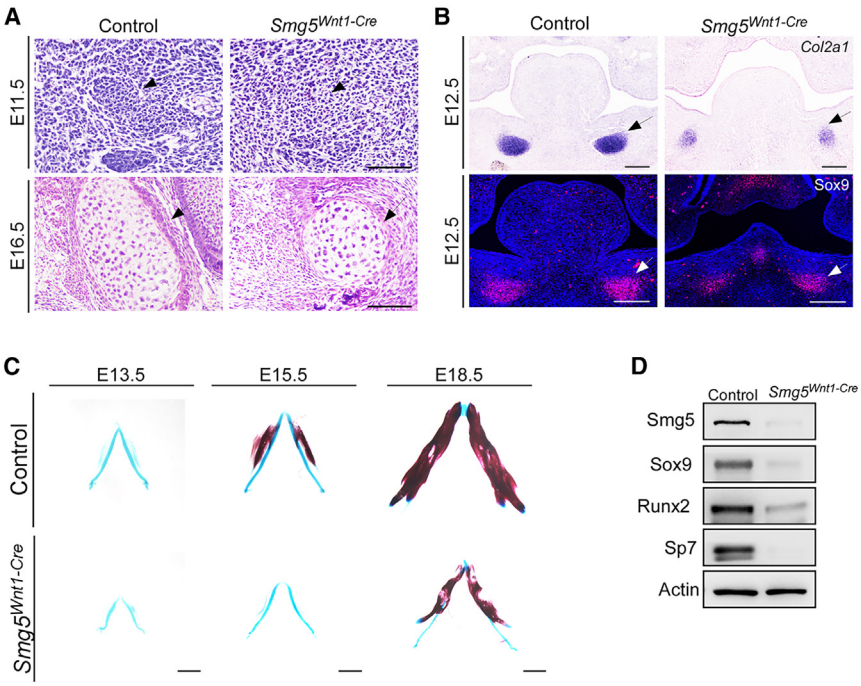

Figure 4. Loss of *Smg5* in CNCCs compromises chondrogenesis and osteogenesis in developing mandibles

(A) Histological analyses of frontal sections show mesenchymal cell condensation of Meckel's cartilage in control but not in *Smg5*$^{Wnt1\text{-}Cre}$ embryos at E11.5. The size of Meckel's cartilage is significantly reduced in E16.5 *Smg5*$^{Wnt1\text{-}Cre}$ embryos. The presumptive Meckel's cartilage areas and Meckel's cartilage are indicated by arrows.

(B) *In situ* hybridization analysis and immunohistofluorescence analysis show that the expression of chondrogenic markers *Col2a1* and Sox9 is decreased in *Smg5*-deficient mandibles at E12.5.

(C) Skeletal preparations with alizarin red (bone) and Alcian Blue (cartilage) shows reduced Meckel's cartilage size and impaired bone formation in developing *Smg5*$^{Wnt1\text{-}Cre}$ mandibles.

(D) Western blotting reveals that the level of osteogenic markers, Runx2 and Sp7, and the chondrogenic marker Sox9, is dramatically decreased in *Smg5*$^{Wnt1\text{-}Cre}$ mandibles at E13.5. β-Actin was used as a loading control. Scale bars: 100 μm in (A), 200 μm in (B), and 1 mm in (C).

accumulation of undegraded NMD target genes. In the Venn diagram of DETs across the developmental stages from E11.5 to E13.5, 1564 transcripts were found to be upregulated in all three stages (Figure S4). Conversely, 70 transcripts were consistently downregulated throughout these stages. Additionally, a small subset of DETs exhibited inconsistent expression changes across the three stages. Some were upregulated followed by downregulation, while others showed the opposite pattern. Some displayed even more complex patterns, indicating the intricate interplay between gene expression dynamics and the regulatory mechanisms influenced by NMD inactivation during embryonic development. These complex patterns may be associated with genes that undergo alternative splicing, which have multiple isoforms showing different expression trends under NMD inactivation.

Next, we performed enrichment analysis using Enrichr, a suite of gene set enrichment analysis tools,[29] with genes containing DETs from E10.5 to E13.5, and similar results were obtained in these three stages; shown are the results from E11.5 (Figures 6C and 6D). Analysis against the MGI_Mammalian Phenotype library revealed that they were mostly enriched in the preweaning lethality and embryonic lethality during organogenesis gene sets (Figure 6C), suggesting a fundamental role for Smg5 in regulating mammalian embryonic and fetal development. GO_Molecular_function analysis revealed that DETs are most significantly enriched in functions related to RNA binding and mRNA binding, including serine/arginine (SR)-rich proteins (also known as SR splicing factors, Srsfs) and heterogeneous nuclear ribonucleoproteins (hnRNPs) (Figure 6D; Table S5). The changes in these RNA-binding DETs are highly complex. For instance, at E11.5, the protein-coding transcript of *Srsf1* is downregulated by up to 2.4-fold as shown in Table S5. Transcripts of *Hnrnph1*, *Hnrnp3*, and *Hnrnpl* that contain PTCs are significantly upregulated, with increases of 13.36-fold, 8.95-fold, and 13.27-fold, respectively. *Hnrnpk* shows significant expression changes in seven transcripts encoding full-length proteins: two are upregulated by 19.77-fold and 21.83-fold, while five are downregulated ranging from 2.65-fold to 14.86-fold. This result is in support of the previous notion that spicing factors used alternative splicing and NMD for regulating the outcome of their expression and could account for the altered alternative splicing events in *Smg5*$^{Wnt1\text{-}Cre}$. The expression of several genes encoding RNA-binding proteins, which are well-known NMD targets, is also confirmed by our RT-PCR data (Figures 5A and 5B). Chromatin immunoprecipitation (ChIP) enrichment analysis (ChEA) revealed that the DETs are strongly associated with genes that are putative targets of RUNX2, a transcription factor essential for osteoblast differentiation (Figure 6E). This result, together with our skeletal staining and western blot results (Figure 4C), suggests that osteoblast differentiation is severely impaired in *Smg5*$^{Wnt1\text{-}Cre}$ mice.

To explore the key molecules that are involved in the formation of cleft palate in *Smg5*$^{Wnt1\text{-}Cre}$, we performed Venn analysis of genes that enriched in abnormal craniofacial morphology gene sets of three embryonic stages, and the results revealed 14 genes that exhibit DETs at all the three stages (Figure 6F). Further analysis showed that only 10 transcripts of the 14 genes are constantly changed from E10.5 to E13.5 (Figure 6G). To further identify the most plausible target gene contributing to the phenotypic defects observed in *Smg5*-deficient mice, we examined the functional roles of these consistently altered genes. Through a thorough literature review, we found that *Porcn* is required for palmitoylation modification of WNT ligands for functioning and its deficiency is associated with cleft palate.[10] In contrast, the

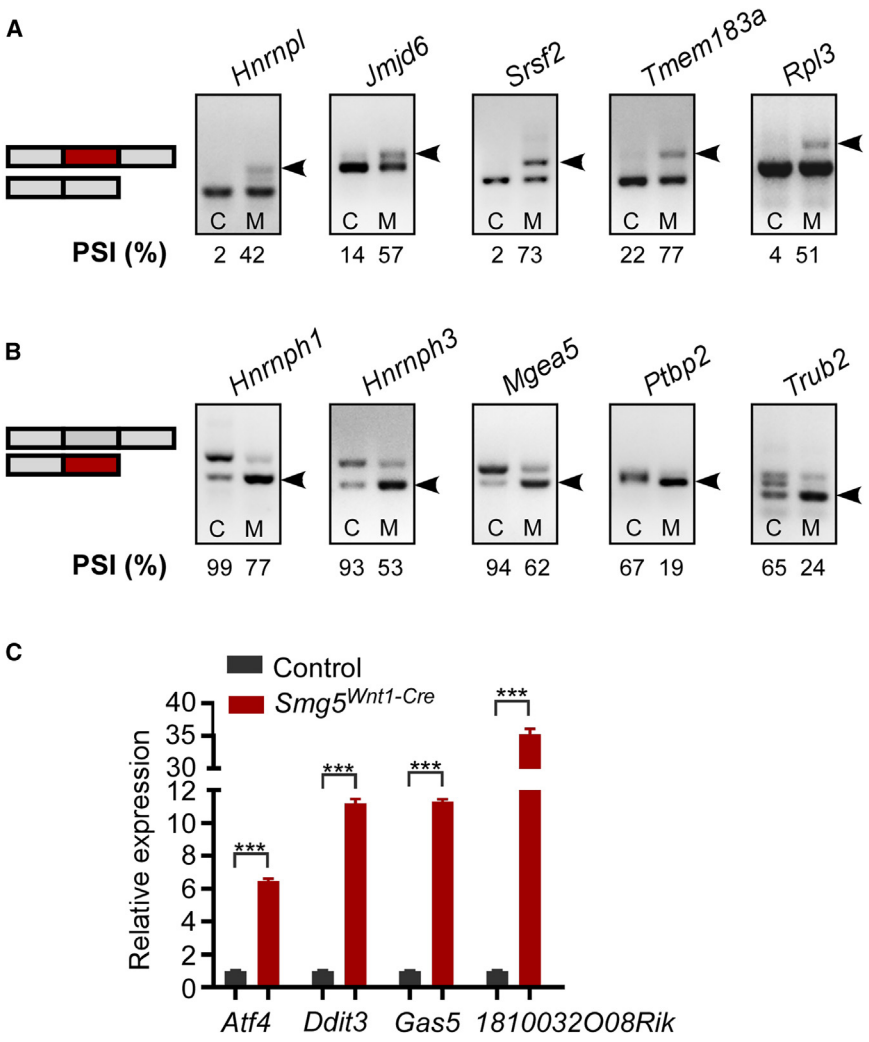

Figure 5. Deletion of *Smg5* with *Wnt1-Cre* leads to impaired NMD activity

(A and B) RT-PCR analysis reveals significant alterations in the alternative splicing of established NMD targets in *Smg5*$^{Wnt1\text{-}Cre}$ mandibles. Arrows highlight potential PTC-containing isoforms that exhibit increased levels following *Smg5* depletion. The percent spliced-in (PSI) values for each gene are displayed below the corresponding RT-PCR images.

(C) Quantitative RT-PCR analysis showing significantly increased expression of NMD target genes including *Atf4*, *Ddit3*, *Gas5*, and 1810032O08Rik in *Smg5*-deficient mandibles. Data were shown as mean ± SEM. Student's t test, ***$p < 0.001$. C, control; M, *Smg5*$^{Wnt1\text{-}Cre}$.

other genes showed no significant association with craniofacial development or cleft palate. Based on these findings, we identified *Porcn* as a potential key target regulated by *Smg5*-mediated NMD.

Porcn is the key target of Smg5-mediated NMD in regulating mouse craniofacial development

Subsequently, we investigated whether the dysregulation of *Porcn* expression was the principal factor behind the observed phenotypes in *Smg5*$^{Wnt1\text{-}Cre}$ mice. We performed Integrative Genomics Viewer visualization analysis on the RNA sequencing data of *Porcn* gene expression at E11.5. As revealed by the Sashimi plot, the inclusion levels of exons 3 through 7 in the *Porcn* gene are significantly reduced in *Smg5*$^{Wnt1\text{-}Cre}$ embryos (Figure 7A). This decrease in exon inclusion was consistent from E11.5 to E13.5, suggesting a sustained impact of *Smg5* deficiency on *Porcn* splicing (Figure S5A). The RNA sequencing results also show that the *Porcn* gene produces multiple isoforms during development, with the NM_016913 isoform, which encodes a normal protein, predominating in wild-type embryos (Figure S5B). In *Smg5* knockout mice, however, the PTC-containing isoform (T013571) became the main expression variant (Figures 7B, 7C, and S5B). Conversely, the level of NM_016913 encoding the full-length Porcn protein was significantly downregulated in *Smg5*$^{Wnt1\text{-}Cre}$ mandibles from E11.5 (Figures 7B, 7C, and S5B). These results from RNA-seq were further confirmed by RT-PCR analysis (Figure 7D). Similar results were observed in maxillary samples (Figure S6). Moreover, western blot analysis revealed that the altered alternative splicing events of *Porcn* leads to significantly decreased Porcn protein (Figure 7E). *Wnt5a* is expressed in the CNCCs-derived mesenchyme, and *Wnt5a* knockout leads to cleft palate.[8] Like other Wnts, palmitoylation by Porcn on Wnt5a is necessary for its activity.[30] Wnt5a acts through the non-canonical Wnt (JNK/c-Jun) signaling[31]; thus, we next investigated whether the Wnt5a/JNK signaling pathway was affected in *Smg5*$^{Wnt1\text{-}Cre}$ mandibles because of abnormal *Porcn* expression. Western blot analysis revealed that the phosphorylation level of JNK was greatly decreased in *Smg5*$^{Wnt1\text{-}Cre}$ mandibles (Figure 7E), indicating an impaired Wnt5a/JNK signaling activity. Finally, we investigated whether Wnt5a would counteract the craniofacial defects caused by *Smg5* knockout. Interestingly, the introduction of Wnt5a recombinant protein to *in vitro* explants of CNCs evidently rescued the cell death of *Smg5*$^{Wnt1\text{-}Cre}$ CNCs (Figure 7F). These data indicate that *Porcn* is the key target of *Smg5*-NMD in CNCCs-derived mesenchyme in mouse craniofacial development.

DISCUSSION

Although the role of Smg5 in the NMD machinery has been reported,[15–17] little is known about its developmental relevance. In the present study, we address the question of whether and how Smg5-mediated NMD is involved in craniofacial development. Craniofacial tissues are derived primarily from CNCCs,

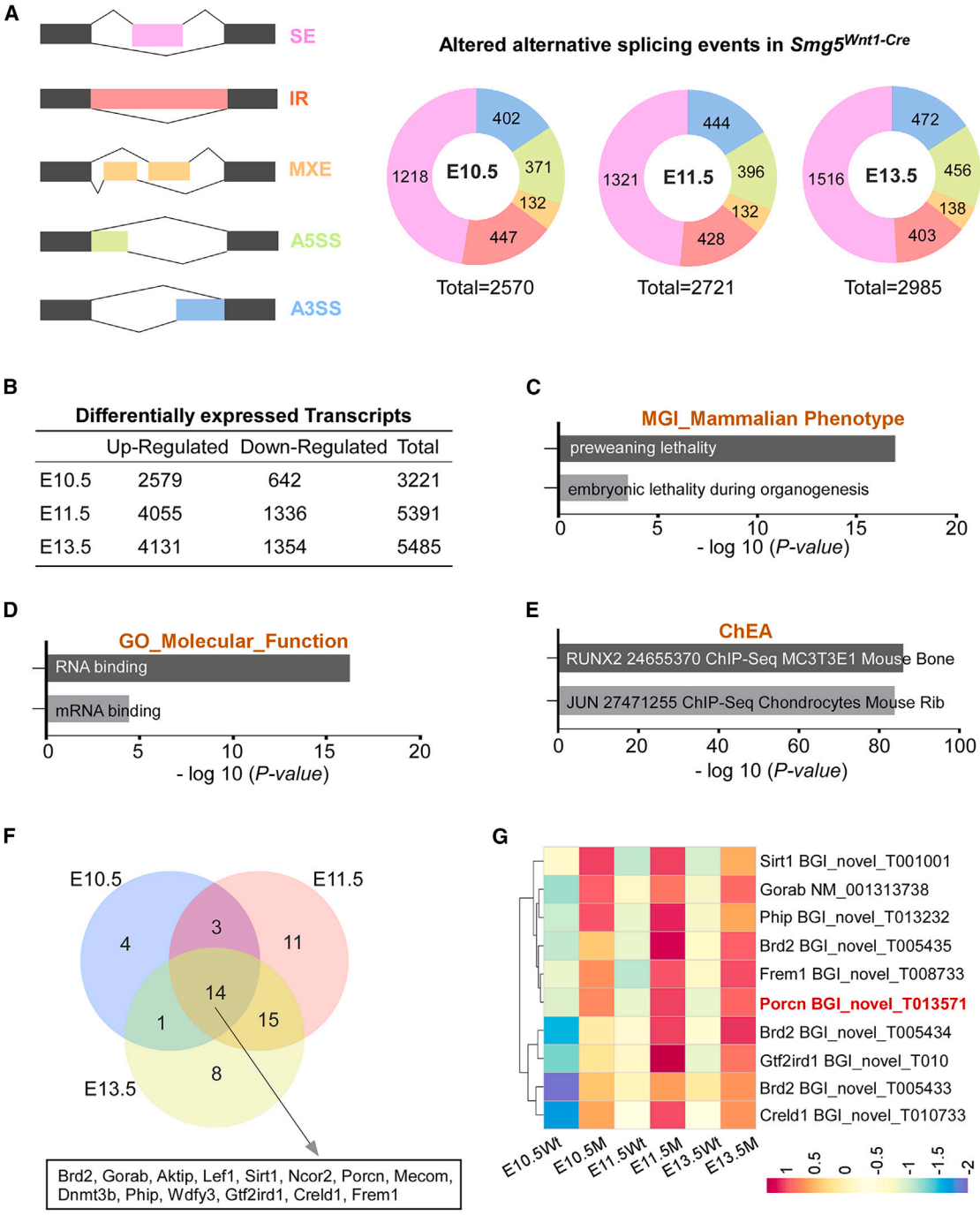

Figure 6. *Smg5* deficiency results in altered alternative splicing events

(A) RNA-seq analysis reveals significant alterations in alternative splicing patterns in *Smg5*$^{Wnt1\text{-}Cre}$ mandibles. The left panel presents schematic diagrams illustrating the five fundamental types of alternative splicing: skipped exon (SE), intron retention (IR), mutually exclusive exons (MXE), alternative 5′ splice sites (A5SS), and alternative 3′ splice sites (A3SS). The corresponding donut charts to the right display the number of genes exhibiting differential alternative splicing for each of the five categories in developing *Smg5*$^{Wnt1\text{-}Cre}$ mandibles.

(B) Table showing numbers of significantly upregulated and downregulated transcripts in *Smg5*-deficient mandibles at various stages.

(C–E) Enrichment analysis of differentially expressed transcripts at E11.5 revealed that Smg5 function is strongly associated with RNA binding, preweaning lethality, and osteogenesis and chondrogenesis.

(F) Venn analysis of genes with differentially expressed transcripts that involved in regulating craniofacial morphology in *Smg5*$^{Wnt1\text{-}Cre}$ mandibles at E10.5, E11.5, and E13.5.

(G) Heatmap analysis of the differentially expressed transcripts that constantly changed in *Smg5*$^{Wnt1\text{-}Cre}$ mandibles at E10.5, E11.5, and E13.5.

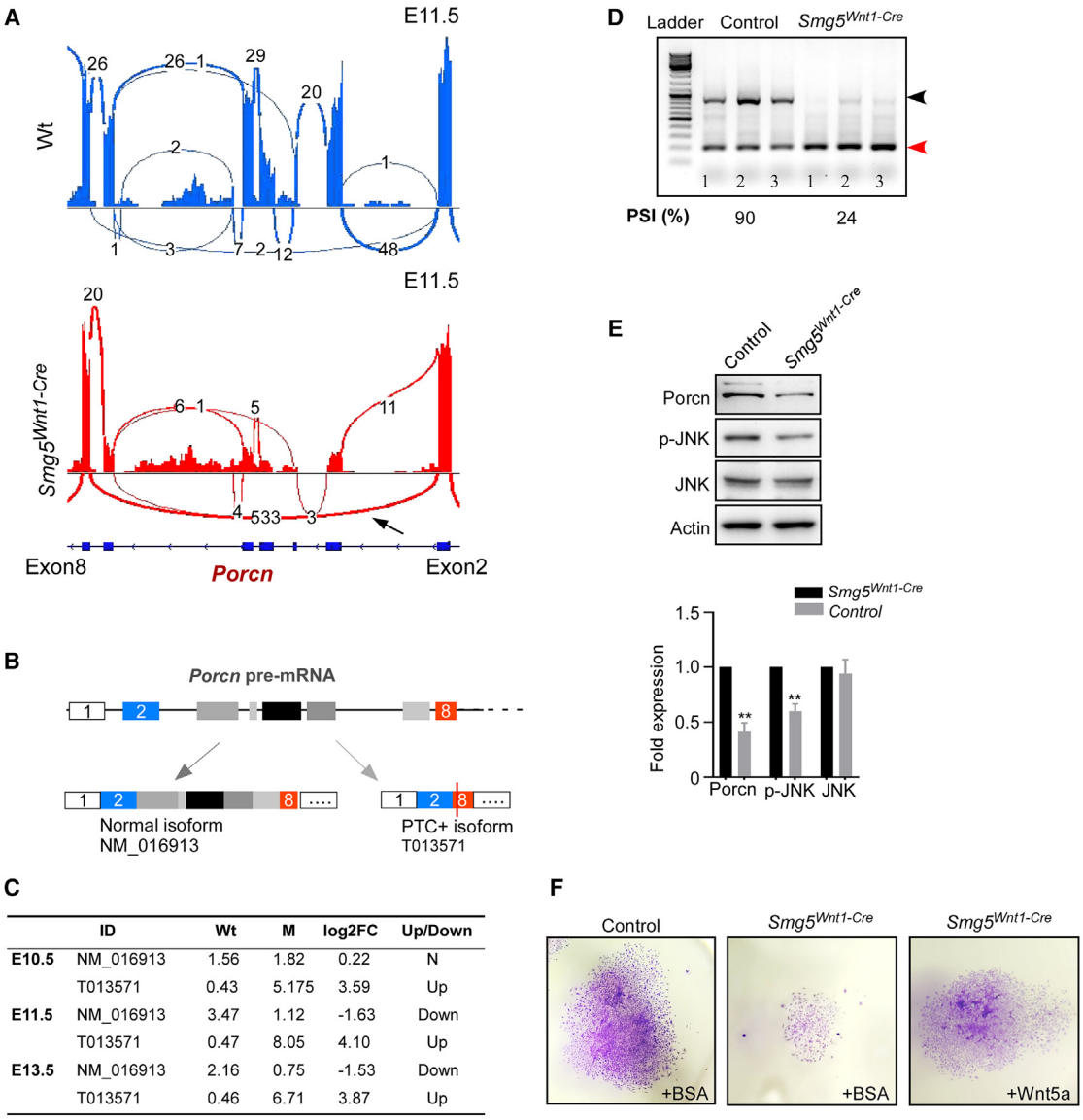

	ID	Wt	M	log2FC	Up/Down
E10.5	NM_016913	1.56	1.82	0.22	N
	T013571	0.43	5.175	3.59	Up
E11.5	NM_016913	3.47	1.12	-1.63	Down
	T013571	0.47	8.05	4.10	Up
E13.5	NM_016913	2.16	0.75	-1.53	Down
	T013571	0.46	6.71	3.87	Up

Figure 7. Post-transcriptional regulation of *Porcn* by Smg5-mediated NMD regulates craniofacial development in mice

(A) A Sashimi plot reveals a significant reduction in the inclusion levels of exons 3–7 of *Porcn* in *Smg5*$^{Wnt1\text{-}Cre}$ mandibles (indicated by an arrow).

(B) Schematic representation of *Porcn* alternative splicing. The PTC-containing isoform lacking exons 3–7.

(C) Table showing the level of main *Porcn* transcripts during mandible development.

(D) RT-PCR analysis showing decreased normal isoform level and increased PTC-containing isoform level in mandibles lacking *Smg5* at E13.5. The percent spliced-in (PSI) values for *Porcn* are displayed below the RT-PCR image.

(E) Western blotting reveals that the levels of Porcn and the downstream phosphorylated JNK are dramatically decreased in *Smg5*-depletion mandibles at E13.5. Statistical analysis of western blot bands reveals a significant reduction in Porcn and *p*-JNK in *Smg5*-deficent tissues.

(F) Addition of Wnt5a attenuates the cell death of CNCCs that migrated from *Smg5*$^{Wnt1\text{-}Cre}$ CNC explants. CNCs from control and *Smg5*$^{Wnt1\text{-}Cre}$ embryos were dissected at E8.5, subjected to *in vitro* organ culture, collected at day 9, and stained by crystal violet ($n = 3$). Recombinant Wnt5a (0.2 μg/mL) or BSA was added to the culture medium 24 h after dissection. Data were shown as mean ± SEM. Student's t test, $^{**}p < 0.01$. M, *Smg5*$^{Wnt1\text{-}Cre}$.

and defective CNCC development often leads to cleft palate[3,6,32]; thus, the regulation of CNCCs development is of great significance for understanding the molecular mechanism governing craniofacial development. In this study, we show that *Smg5*-mediated NMD is required for the differentiation of CNCCs during mouse embryonic development.

Mutation of *SMG9*, encoding an essential component of the SMG1-Upf1-eRF1-eRF3 (SURF) complex that generates phospho-UPF1, also leads to multiple congenital anomalies syndrome including craniofacial dysmorphism in humans.[24] NMD degrades transcripts containing PTCs relying on RNA splicing and the assistance of components in the exon junction complex

(EJC), including *EIF4A3*, *MAGOH*, or *RBM8A*.[33] Mutations in these EJC components are associated with craniofacial disorders.[34–36] For example, *EIF4A3* mutations lead to Richieri-Costa-Pereira syndrome in humans, marked by craniofacial and limb abnormalities.[34] In zebrafish, *eif4a3* knockdown results in underdeveloped craniofacial structures, similar to the human syndrome.[34] Haploinsufficiency for *Eif4a3*, *Magoh*, or *Rbm8a* leads to aberrant neurogenesis and microcephaly through p53 signaling in mice.[36] In addition to our findings that *Smg5* deficiency leads to cleft palate and micrognathia in mice, these findings suggest an essential role of key genes in the NMD pathway in vertebrate craniofacial development.

Elevation of palatal shelves from a vertical to a horizontal position coincides precisely with specific morphogenetic changes in other orofacial organs.[5] The palatal shelves of $Smg5^{Wnt1\text{-}Cre}$ fail to elevate at E14.5 and result in cleft palate. In mammals, Meckel's cartilage regulates the extension of the mandible and the growth of the primary ossification center of the mandible.[25,37] Thus, the small mandible of $Smg5^{Wnt1\text{-}Cre}$ probably results from its severely shortened Meckel's cartilage.

NMD plays a critical role in regulating stem cell differentiation: *Smg6* knockout results in sustained expression of pluripotency genes and inhibition of embryonic stem cell differentiation.[15] Additionally, a global differentiation defect has been observed in *Smg5*, *Smg6*, and *Smg7*-deficient embryonic stem cells (ESCs).[16,38] In support of these results, our results show that both chondrogenic and osteogenic cell differentiation are severely compromised in response to *Smg5* loss. Furthermore, we found that WNT5A could restore cell viability in *Smg5*-deficient CNC explants, suggesting that the increased cell apoptosis in $Smg5^{Wnt1\text{-}Cre}$ may have occurred to eliminate cells with a failure in differentiation.

Most mammalian genes undergo alternative splicing to increase proteomic diversity, generating productive isoforms that code for functional proteins, while unproductive isoforms containing PTCs are targeted for degradation.[12,39,40] Approximately one-third of alternative splicing events generate transcripts containing PTCs that are targeted for degradation by NMD in humans.[12] This coupling of alternative splicing with NMD fine-tunes the balance of mRNAs encoding functional proteins versus those harboring PTCs within a single gene locus.[40] Notably, numerous RNA-binding proteins, such as *Hnrnpl*, *Ptbp2*, *Srsf1*, and *Rpl3*, which are pivotal in mRNA splicing regulation, employ alternative splicing and NMD to modulate their own mRNA levels through a feedback loop mechanism. In *Caenorhabditis elegans*, it has been shown that *smg* genes can influence the expression of normal genes by altering the levels of alternatively spliced mRNAs of SRp20 and SRp30b.[41] Similarly, in *Smg6* knockout mouse embryonic stem cells, the alternative splicing of several splicing factors, including *Rps12*, *Srsf2*, and *Hnrnph1*, is disrupted.[15] Consistent with these findings, our study reveals that *Smg5* knockout profoundly affects the alternative splicing of RNA-binding proteins. It is reasonable to infer that the changes in RNA-binding proteins are associated with the splicing and gene expression alterations induced by *Smg5* knockout, suggesting that the misregulation of RNA-binding proteins could largely contribute to the mRNA expression disruptions caused by *Smg5* deficiency.

Here we identify *Porcn* as a key target of NMD in regulating mandible development. In addition to the retaining of the PTC-containing isoform, the normal isoform of *Porcn* is also significantly decreased due to *Smg5* deficiency. Although the molecular mechanism for regulating the alternative splicing of *Porcn* is unclear, *Porcn* transcripts have been identified to be associated with RNA-binding protein HnRNPK in cultured rat hippocampal neurons.[42] Additionally, RNA immunoprecipitation sequencing (RIP-seq) analysis indicates a potential interaction between HnRNPL and *PORCN* pre-mRNA in prostate cancer LNCaP cells.[43] Our results reveal that impaired NMD results in the deregulation of these HnRNP proteins. Specifically, the PTC-containing isoform of *Hnrnpl* is markedly upregulated in response to *Smg5* loss. In the case of *Hnrnpk*, the transcriptional changes are variable, with some transcripts increasing and others decreasing. Thus, the decrease of *Porcn* normal isoforms may be resulted from the dysregulated splicing regulators upon NMD ablation. It would be interesting to elucidate which alternative splicing regulator is coupled with NMD for maintaining the normal level of *Porcn* during embryonic development in further studies.

In this report, we provide a novel molecular mechanism for the fine-tuning of mesenchymal Wnt signaling activity by regulation of *Porcn* with alternative splicing and NMD during embryonic development. Given the significant role of Wnt signaling in development and disease, it is worthy to investigate whether the regulation of *Porcn* expression level by NMD represents a common molecular mechanism in fine-tuning of Wnt signaling level in other organs or in disease.

Limitations of the study

Our study elucidates the pivotal role of *Smg5*-mediated NMD in craniofacial development of mice. Specifically, we have discovered that *Smg5*-dependent NMD modulates the Wnt signaling cascade by regulating the alternative splicing outcome of *Porcn*, thereby influencing craniofacial development. While our findings provide valuable insights, we have not yet identified the specific RNA-binding proteins whose altered expression in *Smg5*-deficient tissues leads to dysregulation in *Porcn* expression. Furthermore, it remains unclear whether the changes in *Porcn* splicing are a direct consequence of NMD's impact on a single RNA-binding protein or if they result from a complex interplay among multiple splicing regulators. Future studies should aim to address these gaps in knowledge, providing a more comprehensive understanding of the intricate interplay between Smg5-mediated NMD, *Porcn* splicing, Wnt signaling, and craniofacial morphogenesis.

RESOURCE AVAILABILITY

Lead contact

Further information and requests for resources and reagents should be directed to the lead contact, Xiao-Jing Zhu (xiao_jingzhu@hznu.edu.cn).

Materials availability

This study did not generate new unique materials or reagents.

Data and code availability

- The RNA-seq data have been deposited in the Genome Sequence Archive (GSA) of the National Genomics Data Center, China National

Center for Bioinformation/Beijing Institute of Genomics, Chinese Academy of Sciences, and is publicly accessible as of the date of publication. Accession number is listed in the key resources table.
- This paper does not report original code.
- Any additional information required to reanalyze the data reported in this paper is available from the lead contact upon request.

ACKNOWLEDGMENTS

This work was supported by the Zhejiang Provincial Natural Science Foundation of China (ZJNSF) (Grant No. LY22C050003, LY24C090007).

AUTHOR CONTRIBUTIONS

S.Z., **S.H.** contributed to design, data acquisition, and interpretation; **W.H., C.H., J.Z.**, **X.J.** contributed to data acquisition, verification, and interpretation; **Y.Q., C.C., Z.-M.D., X.Y., M.Q.** contributed to data interpretation; **T.L.** contributed to conception, design, data acquisition, and interpretation; **X.-J.Z.** contributed to conception, design, data interpretation, and supervision. All authors were involved in drafting or revising the manuscript and gave final approval and agree to be accountable for all aspects of the work.

DECLARATION OF INTERESTS

The authors declare that they have no competing interests.

STAR★METHODS

Detailed methods are provided in the online version of this paper and include the following:

- KEY RESOURCES TABLE
- EXPERIMENTAL MODEL AND STUDY PARTICIPANT DETAILS
  - Ethics statement
  - Animals
- METHOD DETAILS
  - Histology, immunohistochemistry, *in situ* hybridization, Alcian blue and alizarin red staining, and western blotting
  - Cell apoptosis assays
  - RT–PCR
  - RNA-seq analysis
  - *In vitro* organ culture
- QUANTIFICATION AND STATISTICAL ANALYSIS

SUPPLEMENTAL INFORMATION

Supplemental information can be found online at https://doi.org/10.1016/j.isci.2025.111972.

Received: July 30, 2024
Revised: October 21, 2024
Accepted: February 4, 2025
Published: February 6, 2025

REFERENCES

1. Iwaya, C., Suzuki, A., and Iwata, J. (2023). MicroRNAs and Gene Regulatory Networks Related to Cleft Lip and Palate. Int. J. Mol. Sci. *24*, 3552. https://doi.org/10.3390/ijms24043552.
2. Trainor, P.A. (2005). Specification and patterning of neural crest cells during craniofacial development. Brain Behav. Evol. *66*, 266–280. https://doi.org/10.1159/000088130.
3. Liao, J., Huang, Y., Wang, Q., Chen, S., Zhang, C., Wang, D., Lv, Z., Zhang, X., Wu, M., and Chen, G. (2022). Gene regulatory network from cranial neural crest cells to osteoblast differentiation and calvarial bone development. Cell. Mol. Life Sci. *79*, 158. https://doi.org/10.1007/s00018-022-04208-2.
4. Sweat, Y.Y., Sweat, M., Yu, W., Sanz-Navarro, M., Zhang, L., Sun, Z., Eliason, S., Klein, O.D., Michon, F., Chen, Z., and Amendt, B.A. (2020). Sox2 Controls Periderm and Rugae Development to Inhibit Oral Adhesions. J. Dent. Res. *99*, 1397–1405. https://doi.org/10.1177/0022034520939013.
5. Nohara, A., Owaki, N., Matsubayashi, J., Katsube, M., Imai, H., Yoneyama, A., Yamada, S., Kanahashi, T., and Takakuwa, T. (2022). Morphometric analysis of secondary palate development in human embryos. J. Anat. *241*, 1287–1302. https://doi.org/10.1111/joa.13745.
6. Dash, S., Bhatt, S., Falcon, K.T., Sandell, L.L., and Trainor, P.A. (2021). Med23 Regulates Sox9 Expression during Craniofacial Development. J. Dent. Res. *100*, 406–414. https://doi.org/10.1177/0022034520969109.
7. Reynolds, K., Kumari, P., Sepulveda Rincon, L., Gu, R., Ji, Y., Kumar, S., and Zhou, C.J. (2019). Wnt signaling in orofacial clefts: crosstalk, pathogenesis and models. Dis. Model. Mech. *12*, dmm037051. https://doi.org/10.1242/dmm.037051.
8. He, F., Xiong, W., Yu, X., Espinoza-Lewis, R., Liu, C., Gu, S., Nishita, M., Suzuki, K., Yamada, G., Minami, Y., and Chen, Y. (2008). Wnt5a regulates directional cell migration and cell proliferation via Ror2-mediated noncanonical pathway in mammalian palate development. Development *135*, 3871–3879. https://doi.org/10.1242/dev.025767.
9. Liu, Y., Wang, M., Zhao, W., Yuan, X., Yang, X., Li, Y., Qiu, M., Zhu, X.J., and Zhang, Z. (2015). Gpr177-mediated Wnt Signaling Is Required for Secondary Palate Development. J. Dent. Res. *94*, 961–967. https://doi.org/10.1177/0022034515583532.
10. Bankhead, E.J., Colasanto, M.P., Dyorich, K.M., Jamrich, M., Murtaugh, L.C., and Fuhrmann, S. (2015). Multiple requirements of the focal dermal hypoplasia gene porcupine during ocular morphogenesis. Am. J. Pathol. *185*, 197–213. https://doi.org/10.1016/j.ajpath.2014.09.002.
11. Han, X., Wei, Y., Wang, H., Wang, F., Ju, Z., and Li, T. (2018). Nonsense-mediated mRNA decay: a 'nonsense' pathway makes sense in stem cell biology. Nucleic Acids Res. *46*, 1038–1051. https://doi.org/10.1093/nar/gkx1272.
12. Lewis, B.P., Green, R.E., and Brenner, S.E. (2003). Evidence for the widespread coupling of alternative splicing and nonsense-mediated mRNA decay in humans. Proc. Natl. Acad. Sci. USA *100*, 189–192. https://doi.org/10.1073/pnas.0136770100.
13. Kurosaki, T., Popp, M.W., and Maquat, L.E. (2019). Quality and quantity control of gene expression by nonsense-mediated mRNA decay. Nat. Rev. Mol. Cell Biol. *20*, 406–420. https://doi.org/10.1038/s41580-019-0126-2.
14. Huang, L., Shum, E.Y., Jones, S.H., Lou, C.H., Chousal, J., Kim, H., Roberts, A.J., Jolly, L.A., Espinoza, J.L., Skarbrevik, D.M., et al. (2018). A Upf3b-mutant mouse model with behavioral and neurogenesis defects. Mol. Psychiatr. *23*, 1773–1786. https://doi.org/10.1038/mp.2017.173.
15. Li, T., Shi, Y., Wang, P., Guachalla, L.M., Sun, B., Joerss, T., Chen, Y.S., Groth, M., Krueger, A., Platzer, M., et al. (2015). Smg6/Est1 licenses embryonic stem cell differentiation via nonsense-mediated mRNA decay. EMBO J. *34*, 1630–1647. https://doi.org/10.15252/embj.201489947.
16. Huth, M., Santini, L., Galimberti, E., Ramesmayer, J., Titz-Teixeira, F., Sehlke, R., Oberhuemer, M., Stummer, S., Herzog, V., Garmhausen, M., et al. (2022). NMD is required for timely cell fate transitions by fine-tuning gene expression and regulating translation. Gene Dev. *36*, 348–367. https://doi.org/10.1101/gad.347690.120.
17. Boehm, V., Kueckelmann, S., Gerbracht, J.V., Kallabis, S., Britto-Borges, T., Altmüller, J., Krüger, M., Dieterich, C., and Gehring, N.H. (2021). SMG5-SMG7 authorize nonsense-mediated mRNA decay by enabling SMG6 endonucleolytic activity. Nat. Commun. *12*, 3965. https://doi.org/10.1038/s41467-021-24046-3.
18. McIlwain, D.R., Pan, Q., Reilly, P.T., Elia, A.J., McCracken, S., Wakeham, A.C., Itie-Youten, A., Blencowe, B.J., and Mak, T.W. (2010). Smg1 is

required for embryogenesis and regulates diverse genes via alternative splicing coupled to nonsense-mediated mRNA decay. Proc. Natl. Acad. Sci. USA *107*, 12186–12191. https://doi.org/10.1073/pnas.1007336107.

19. Medghalchi, S.M., Frischmeyer, P.A., Mendell, J.T., Kelly, A.G., Lawler, A.M., and Dietz, H.C. (2001). Rent1, a trans-effector of nonsense-mediated mRNA decay, is essential for mammalian embryonic viability. Hum. Mol. Genet. *10*, 99–105. https://doi.org/10.1093/hmg/10.2.99.
20. Weischenfeldt, J., Damgaard, I., Bryder, D., Theilgaard-Mönch, K., Thoren, L.A., Nielsen, F.C., Jacobsen, S.E.W., Nerlov, C., and Porse, B.T. (2008). NMD is essential for hematopoietic stem and progenitor cells and for eliminating by-products of programmed DNA rearrangements. Gene Dev. *22*, 1381–1396. https://doi.org/10.1101/gad.468808.
21. Chousal, J.N., Sohni, A., Vitting-Seerup, K., Cho, K., Kim, M., Tan, K., Porse, B., Wilkinson, M.F., and Cook-Andersen, H. (2022). Progression of the pluripotent epiblast depends upon the NMD factor UPF2. Development *149*, dev200764. https://doi.org/10.1242/dev.200764.
22. Guerra, G.M., May, D., Kroll, T., Koch, P., Groth, M., Wang, Z.Q., Li, T.L., and Grigaravičius, P. (2021). Cell Type-Specific Role of RNA Nuclease SMG6 in Neurogenesis. Cells *10*, 3365. https://doi.org/10.3390/cells10123365.
23. Bao, J.Q., Vitting-Seerup, K., Waage, J., Tang, C., Ge, Y., Porse, B.T., and Yan, W. (2016). UPF2-Dependent Nonsense-Mediated mRNA Decay Pathway Is Essential for Spermatogenesis by Selectively Eliminating Longer 3 ' UTR Transcripts. Plos Genet *12*. ARTN e1005863. PLoS Genet. *12*, e1005863. https://doi.org/10.1371/journal.pgen.1005863.
24. Shaheen, R., Anazi, S., Ben-Omran, T., Seidahmed, M.Z., Caddle, L.B., Palmer, K., Ali, R., Alshidi, T., Hagos, S., Goodwin, L., et al. (2016). Mutations in SMG9, Encoding an Essential Component of Nonsense-Mediated Decay Machinery, Cause a Multiple Congenital Anomaly Syndrome in Humans and Mice. Am. J. Hum. Genet. *98*, 643–652. https://doi.org/10.1016/j.ajhg.2016.02.010.
25. Svandova, E., Anthwal, N., Tucker, A.S., and Matalova, E. (2020). Diverse Fate of an Enigmatic Structure: 200 Years of Meckel's Cartilage. Front. Cell Dev. Biol. *8*, 821. https://doi.org/10.3389/fcell.2020.00821.
26. Ducy, P., Zhang, R., Geoffroy, V., Ridall, A.L., and Karsenty, G. (1997). Osf2/Cbfa1: a transcriptional activator of osteoblast differentiation. Cell *89*, 747–754. https://doi.org/10.1016/s0092-8674(00)80257-3.
27. Otto, F., Thornell, A.P., Crompton, T., Denzel, A., Gilmour, K.C., Rosewell, I.R., Stamp, G.W., Beddington, R.S., Mundlos, S., Olsen, B.R., et al. (1997). Cbfa1, a candidate gene for cleidocranial dysplasia syndrome, is essential for osteoblast differentiation and bone development. Cell *89*, 765–771. https://doi.org/10.1016/s0092-8674(00)80259-7.
28. Nakashima, K., Zhou, X., Kunkel, G., Zhang, Z., Deng, J.M., Behringer, R.R., and de Crombrugghe, B. (2002). The novel zinc finger-containing transcription factor osterix is required for osteoblast differentiation and bone formation. Cell *108*, 17–29. https://doi.org/10.1016/s0092-8674(01)00622-5.
29. Xie, Z., Bailey, A., Kuleshov, M.V., Clarke, D.J.B., Evangelista, J.E., Jenkins, S.L., Lachmann, A., Wojciechowicz, M.L., Kropiwnicki, E., Jagodnik, K.M., et al. (2021). Gene Set Knowledge Discovery with Enrichr. Curr. Protoc. *1*, e90. https://doi.org/10.1002/cpz1.90.
30. Liu, Y., Qi, X., Donnelly, L., Elghobashi-Meinhardt, N., Long, T., Zhou, R.W., Sun, Y., Wang, B., and Li, X. (2022). Mechanisms and inhibition of Porcupine-mediated Wnt acylation. Nature *607*, 816–822. https://doi.org/10.1038/s41586-022-04952-2.
31. Oishi, I., Suzuki, H., Onishi, N., Takada, R., Kani, S., Ohkawara, B., Koshida, I., Suzuki, K., Yamada, G., Schwabe, G.C., et al. (2003). The receptor tyrosine kinase Ror2 is involved in non-canonical Wnt5a/JNK signalling pathway. Genes Cells *8*, 645–654. https://doi.org/10.1046/j.1365-2443.2003.00662.x.
32. Hammond, N.L., Brookes, K.J., and Dixon, M.J. (2018). Ectopic Hedgehog Signaling Causes Cleft Palate and Defective Osteogenesis. J. Dent. Res. *97*, 1485–1493. https://doi.org/10.1177/0022034518785336.
33. Kervestin, S., and Jacobson, A. (2012). NMD: a multifaceted response to premature translational termination. Nat. Rev. Mol. Cell Biol. *13*, 700–712. https://doi.org/10.1038/nrm3454.
34. Favaro, F.P., Alvizi, L., Zechi-Ceide, R.M., Bertola, D., Felix, T.M., de Souza, J., Raskin, S., Twigg, S.R.F., Weiner, A.M.J., Armas, P., et al. (2014). A Noncoding Expansion in Causes Richieri-Costa-Pereira Syndrome, a Craniofacial Disorder Associated with Limb Defects. Am. J. Hum. Genet. *94*, 120–128. https://doi.org/10.1016/j.ajhg.2013.11.020.
35. Miertus, J., Maltese, P.E., Hyblová, M., Tomková, E., Durovcíková, D., Rísová, V., and Bertelli, M. (2020). Expanding the phenotype of thrombocytopenia absent radius syndrome with hypospadias. J. Biotechnol. *311*, 44–48. https://doi.org/10.1016/j.jbiotec.2020.02.011.
36. Mao, H.Q., McMahon, J.J., Tsai, Y.H., Wang, Z.F., and Silver, D.L. (2016). Haploinsufficiency for Core Exon Junction Complex Components Disrupts Embryonic Neurogenesis and Causes p53-Mediated Microcephaly. PLoS Genet. *12*, e1006282. https://doi.org/10.1371/journal.pgen.1006282.
37. Frommer, J., and Margolies, M.R. (1971). Contribution of Meckel's cartilage to ossification of the mandible in mice. J. Dent. Res. *50*, 1260–1267. https://doi.org/10.1177/00220345710500052801.
38. Chen, C., Wei, Y., Jiang, X., and Li, T. (2024). RNA Surveillance Factor SMG5 Is Essential for Mouse Embryonic Stem Cell Differentiation. Biomolecules *14*, 1023. https://doi.org/10.3390/biom14081023.
39. Wright, C.J., Smith, C.W.J., and Jiggins, C.D. (2022). Alternative splicing as a source of phenotypic diversity. Nat. Rev. Genet. *23*, 697–710. https://doi.org/10.1038/s41576-022-00514-4.
40. Weischenfeldt, J., Waage, J., Tian, G., Zhao, J., Damgaard, I., Jakobsen, J.S., Kristiansen, K., Krogh, A., Wang, J., and Porse, B.T. (2012). Mammalian tissues defective in nonsense-mediated mRNA decay display highly aberrant splicing patterns. Genome Biol. *13*, R35. https://doi.org/10.1186/gb-2012-13-5-r35.
41. Morrison, M., Harris, K.S., and Roth, M.B. (1997). smg mutants affect the expression of alternatively spliced SR protein mRNAs in Caenorhabditis elegans. Proc. Natl. Acad. Sci. USA *94*, 9782–9785. https://doi.org/10.1073/pnas.94.18.9782.
42. Leal, G., Comprido, D., de Luca, P., Morais, E., Rodrigues, L., Mele, M., Santos, A.R., Costa, R.O., Pinto, M.J., Patil, S., et al. (2017). The RNA-Binding Protein hnRNP K Mediates the Effect of BDNF on Dendritic mRNA Metabolism and Regulates Synaptic NMDA Receptors in Hippocampal Neurons. eNeuro *4*, 10. https://doi.org/10.1523/ENEURO.0268-17.2017.
43. Fei, T., Chen, Y., Xiao, T., Li, W., Cato, L., Zhang, P., Cotter, M.B., Bowden, M., Lis, R.T., Zhao, S.G., et al. (2017). Genome-wide CRISPR screen identifies HNRNPL as a prostate cancer dependency regulating RNA splicing. Proc. Natl. Acad. Sci. USA *114*, E5207–E5215. https://doi.org/10.1073/pnas.1617467114.
44. Zhu, S., Huo, S., Wang, Z., Huang, C., Li, C., Song, H., Yang, X., He, R., Ding, C., Qiu, M., and Zhu, X.J. (2024). Follistatin controls the number of murine teeth by limiting TGF-beta signaling. iScience *27*, 110785. https://doi.org/10.1016/j.isci.2024.110785.
45. Belo, J.A., Leyns, L., Yamada, G., and De Robertis, E.M. (1998). The prechordal midline of the chondrocranium is defective in Goosecoid-1 mouse mutants. Mech. Dev. *72*, 15–25. https://doi.org/10.1016/s0925-4773(97)00204-9.
46. Langmead, B., and Salzberg, S.L. (2012). Fast gapped-read alignment with Bowtie 2. Nat. Methods *9*, 357–359. https://doi.org/10.1038/nmeth.1923.
47. Li, B., and Dewey, C.N. (2011). RSEM: accurate transcript quantification from RNA-Seq data with or without a reference genome. BMC Bioinf. *12*, 323. https://doi.org/10.1186/1471-2105-12-323.
48. Florea, L., Song, L., and Salzberg, S.L. (2013). Thousands of exon skipping events differentiate among splicing patterns in sixteen human tissues. F1000Res. *2*, 188. https://doi.org/10.12688/f1000research.2-188.v2.

49. Shen, S., Park, J.W., Lu, Z.X., Lin, L., Henry, M.D., Wu, Y.N., Zhou, Q., and Xing, Y. (2014). rMATS: robust and flexible detection of differential alternative splicing from replicate RNA-Seq data. Proc. Natl. Acad. Sci. USA *111*, E5593–E5601. https://doi.org/10.1073/pnas.1419161111.

50. Chen, E.Y., Tan, C.M., Kou, Y., Duan, Q., Wang, Z., Meirelles, G.V., Clark, N.R., and Ma'ayan, A. (2013). Enrichr: interactive and collaborative HTML5 gene list enrichment analysis tool. BMC Bioinf. *14*, 10. https://doi.org/10.1186/1471-2105-14-128.

51. Kuleshov, M.V., Jones, M.R., Rouillard, A.D., Fernandez, N.F., Duan, Q., Wang, Z., Koplev, S., Jenkins, S.L., Jagodnik, K.M., Lachmann, A., et al. (2016). Enrichr: a comprehensive gene set enrichment analysis web server 2016 update. Nucleic Acids Res. *44*, W90–W97. https://doi.org/10.1093/nar/gkw377.

52. Gonzalez Malagon, S.G., Dobson, L., Munoz, A.M.L., Dawson, M., Barrell, W., Marangos, P., Krause, M., and Liu, K.J. (2019). Dissection, Culture and Analysis of Primary Cranial Neural Crest Cells from Mouse for the Study of Neural Crest Cell Delamination and Migration. J Vis Exp., e60051. https://doi.org/10.3791/60051.

53. Muzumdar, M.D., Tasic, B., Miyamichi, K., Li, L., and Luo, L. (2007). A global double-fluorescent Cre reporter mouse. Genesis *45*, 593–605. https://doi.org/10.1002/dvg.20335.

STAR★METHODS

KEY RESOURCES TABLE

REAGENT or RESOURCE	SOURCE	IDENTIFIER
Antibodies		
Smg5	Abcam	Cat# ab33033; RRID: AB_882612
Sox9	Abcam	Cat# ab185230; RRID: AB_2715497
Runx2	Santa Cruz Biotechnology	Cat# sc-390351; RRID: AB_2892645
Sp7	Abcam	Cat# ab209484; RRID: AB_2892207
Porcn	Abcam	Cat# ab105543; RRID: AB_10860951
p-JNK	Cell Signaling Technology	Cat#4668; RRID: AB_823588
JNK	Cell Signaling Technology	Cat# A4867; RRID: AB_2863367
β-Actin	Cell Signaling Technology	Cat#3700; RRID: AB_2242334
Critical commercial assays		
TUNEL BrightGreen apoptosis detection kit	Vazyme	Cat#A112
RevertAid^{TM} Master Mix	ThermoFischer Scientific	Cat# M1632
UltraSYBR mixture	CWBIO	Cat#E606335
Trizol	ThermoFischer Scientific	Cat# 15596026CN
2xTaq MasterMix	CWBIO	Cat#CW0690
SsoFast EvaGreen Super mix	Bio-Rad	Cat#1725204
Recombinant Wnt5a	R&D	Cat#645-WN; P22725
Deposited data		
RNA-Seq data of developing embryos	This paper	GSA: CRA009091
Experimental models: Organisms/strains		
Mouse: *Smg5*$^{Flox/Flox}$	Dr. Li	Chen et al.[38]
Mouse: *Wnt1-Cre*	The Jackson Laboratory	Cat#004782
Mouse: *ROSA*$^{mT/mG}$	The Jackson Laboratory	Cat#007676
Oligonucleotides		
Genotyping primer for Smg5: Forward: CAGGACTATGAACTGACATGGAGG	This paper	N/A
Genotyping primer for Smg5: Reverse: TACCTCTTAGGGAAAGCTGGGCC	This paper	N/A
Genotyping primer for Cre: Forward: TTCTGCGGGAAACCATTTCCG	This paper	N/A
Genotyping primer for Cre: Reverse: ACTCGCATCACTGCCCTCA	This paper	N/A
RT-PCR primer for Porcn: Forward: CTCCATCTGTCCATCCATCTGT	This paper	N/A
RT-PCR primer for Porcn: Reverse: GCTCCACATTCAACGGTCTA	This paper	N/A
QPCR and RT-PCR primers for NMD targets	Weischenfeldt et al.[20,40]	N/A
Software and algorithms		
GraphPad Prism 9.5	Graphpad Software	http://www.graphpad.com/
Photoshop	Photoshop Software	https://www.adobe.com
Image Lab 5.1	Image Lab Software	Bio-Rad

EXPERIMENTAL MODEL AND STUDY PARTICIPANT DETAILS

Ethics statement

All animal experiments were approved by the Animal Users Committee of Hangzhou Normal University and carried out in strict accordance with the Guide for the Care and Use of Laboratory Animals at Hangzhou Normal University.

Animals

Wnt1-Cre and *ROSA*$^{mT/mG}$ mouse lines were purchased from The Jackson Laboratory (Bar Harbor, ME, USA). Conditional *Smg5* knockout mouse allele was produced by inserting *loxP* sequences flanking exons 2–4 by gene targeting in ESCs with the genetic background of C57BL/6 [38] (Figure S1). *Smg5*$^{f/f}$ mice were crossed with *Wnt1-Cre* mice to generate *Smg5*$^{(f/+);Wnt1\text{-}Cre}$ mice, which were back-crossed with *Smg5*$^{f/f}$ for producing *Smg5* conditional knockout mice (*Smg5*$^{Wnt1\text{-}Cre}$). Primers for genotyping are as follows: *Smg5-F*: 5'- CAGGACTATGAACTGACATGGAGG -3'; *Smg5-R*: 5'- TACCTCTTAGGGAAAGCTGGGCC -3'; *Wnt1-CreF*:5'- TT CTGCGGGAAACCATTTCCG -3'; *Wnt1-CreR*:5'- ACTCGCATCACTGCCCTCA -3'. The PCR bands for WT and alleles are 367 bp and 480 bp, respectively. The PCR bands for *Wnt1-Cre* are 368 bp. The morning of vaginal plug appearance was determined as embryonic day 0 and embryos were harvested from timed pregnant females. Mice at E8.5 and beyond, as well as P0, were used for this study. *Smg5*$^{Wnt1\text{-}Cre}$ mice were compared to their wild-type littermates. Gender does not affect the experimental results, as both female and male *Smg5*$^{Wnt1\text{-}Cre}$ mice exhibit the cleft palate phenotype. All of the available *Smg5*$^{Wnt1\text{-}Cre}$ mice, both male and female, were arbitrarily used for experiments. All the mice used in this study were reared in specific pathogen free (SPF) facilities.

METHOD DETAILS

Histology, immunohistochemistry, *in situ* hybridization, Alcian blue and alizarin red staining, and western blotting

Embryos were dissected and fixed in 4% PFA (Sangon, Shanghai, China) overnight at 4°C. Samples were dehydrated through an ethanol series and embedded in paraffin. After deparaffinization and hydration, 7 μm sections were stained with hematoxylin and eosin (HE) following standard protocols. For *in situ* hybridization, cDNA fragments were cloned into the pGEM®-T Easy vector (Promega), and linearized for probe synthesis. Digoxigenin-labeled probes were generated using T7 or SP6 RNA polymerase (Promega) with DIG RNA Labeling Mix (Roche) and hybridized to 12-μm paraffin sections as previously described.[44] Immunohistofluorescence was performed with 5 μm sections using antibodies against SOX9 (ab185230, Abcam, UK) according to the manufacturer's instructions. For alcian blue and alizarin red staining, embryos were dissected, fixed in 95% ethanol, and stained with alcian blue and alizarin red as described in.[45] For immunoblot analysis, tissue or cell lysates were resolved by SDS-PAGE and subjected to immunoblotting analyses with primary antibodies and the according HRP-linked secondary antibodies according to standard procedures. The following primary antibodies were used for Western blot analysis: Smg5 (ab33033, Abcam), Sox9 (ab185230, Abcam), Runx2 (sc-390351, Santa Cruz Biotechnology), Sp7 (ab209484, Abcam), Porcn (ab105543, Abcam), p-JNK (4668, Cell Signaling Technology), JNK (A4867, Abclonal), and β-Actin (3700, Cell Signaling Technology).

Cell apoptosis assays

Apoptosis was assayed by the Terminal deoxynucleotidyl transferase dUTP nick end labeling (TUNEL) using TUNEL BrightGreen apoptosis detection kit (Vazyme, Nanjing, China) according to the manufacturer's instructions. Briefly, 5-μm-thick paraffin slides were first hydrated, followed by three washes in PBS, treated with 2 mg/ml proteinase K, and balanced with Equilibration Buffer. Then, the sections were incubated with labeling buffer containing BrightGreen Labeling Mix and Recombinant TdT Enzyme and placed in a humidified chamber in the dark at 37°C for 1 h. Finally, the slides were stained with DAPI after three washes of PBS and mounted for fluorescence observation.

RT–PCR

Total RNA from E13.5 mandibles of control and *Smg5*$^{Wnt1\text{-}Cre}$ mice was isolated using Trizol (Thermofisher). cDNA was synthesized from 1 μg of total RNA from each group using RevertAid Master Mix (Thermofisher). For the quantification of NMD target gene expression, qRT–PCR and semi–quantitative RT–PCR was performed in triplicate using SsoFast EvaGreen Super mix (Bio-Rad) and 2xTaq MasterMix (CWBIO), respectively. qRT–PCR was performed in a StepOnePlus™ Real-Time PCR Instrument (Thermo Fisher Scientific). 18S rRNA was used as a reference gene. The 2 -ΔΔCT method was used for quantification of qRT–PCR data. For semi-quantitative RT–PCR analysis to identify the normal and the PTC-containing isoforms, PCR products were examined by electrophoresis through a 2% agarose. PCR primers for NMD common targets were synthesized according to previous publications.[20,40] PCR primers for examining *Porcn* isoforms are: *Porcn-F*: 5'- CTCCATCTGTCCATCCATCTGT -3', and *Porcn-R*: 5'- GCTCCACATT CAACGGTCTA -3'. The PCR bands for NM_016913 and the PTC-containing isoform (T013571) are 880 bp and 204 bp, respectively.

RNA-seq analysis

The mandibles were dissected out from E10.5, E11.5, and E13.5 embryos and subjected to RNA-seq analysis by BGI (Wuhan, China). Briefly, mRNAs were isolated from total RNA with the oligo(dT) method and fragmented for synthesizing first-strand and second-strand cDNA. Subsequently, the cDNA fragments were purified for end repair and single nucleotide A addition, linked with adapters

and selected for PCR amplification for library construction. The samples were sequenced on Illumina Hiseq4000. The clean reads were mapped onto the *Mus musculus* genome (mm10) using Bowtie2 and the gene expression level in each sample was calculated with RSEM.[46,47] Transcripts having probability >0.8 in NOISeq and fold change > 2 were selected as of significant differential expression. ASprofile was used to determine and quantify the alternative splicing events among different samples.[48] Differential alternative splicing events was analyzed by rMATS and an FDR ≦ 0.05 was determined as of significant difference.[49] For each genotype, two independent samples were sequenced respectively. The raw sequence data reported in this paper have been deposited in the Genome Sequence Archive in National Genomics Data Center, China National Center for Bioinformation/Beijing Institute of Genomics, Chinese Academy of Sciences, under accession number CRA009091 that is publicly accessible at https://bigd.big.ac.cn/gsa. Enrichment analysis of RNA-Seq data was performed using Enrichr, which is a comprehensive resource for curated gene sets.[50,51] Donut Chart was generated by Graphpad. Symmetric Venn analysis for genes and Heatmap was performed using the OmicStudio tools. Non-Symmetric Venn analysis for DETs were performed using Draw Venn Diagram (http://bioinformatics.psb.ugent.be/webtools/Venn/). The PSI for well-known NMD targets and *Porcn* is determined utilizing RNA-Seq data. It's calculated by dividing the number of reads that include a particular exon by the total number of reads that either include or skip that exon. Sashimi plot was created utilizing using the Integrative Genomics Viewer (IGV).

In vitro organ culture

For the *in vitro* palate fusion assay, paired palatal shelves from E13.5 embryos were dissected and placed on a Nucleopore Track-Etch Membrane in a Trowell-type organ culture dish for 2 d before harvested for histological analysis. For *in vitro* culture of CNC, E8.5 cranial neural folds were dissected and cultured in gelatin-coated tissue culture dishes in a standard cell culture incubator (37°C, 5% CO_2) as previously described.[52] For observation of the migrated CNCCs, $Smg5^{f/f}$ mice were crossed with $ROSA^{mT/mG}$ Cre reporter mice[53] to carrying the $ROSA^{mT/mG}$ allele. CNC explants from $Smg5^{f/+}$;$ROSA^{mT/mG}$;*Wnt1-Cre* and $Smg5^{f/f}$;$ROSA^{mT/mG}$;*Wnt1-Cre* mice, whose CNCCs were EGFP-positive, were used for fluorescence observation. The fluorescence intensity of CNCCs was analyzed using Photoshop. Fold changes were calculated by normalizing the values to the control at Day2. For Wnt5a rescue experiment, recombinant Wnt5a (0.2 μg/ml, R&D) or BSA (Sangon) were added to the culture medium at 24 hour of dissection and the medium were changed every 3 days. At the 9 days of culture, the CNC explants were fixed by 4% PFA and stained with crystal violet. At least 3 explants were used for analysis for each genotype.

QUANTIFICATION AND STATISTICAL ANALYSIS

Apoptotic cells were counted from three biological replicates for both wild type and mutants within defined areas. Western blot bands were quantified from three independent sample groups using Image Lab (Bio-Rad). The relative protein expression levels were determined by normalizing the gray value of the protein bands to that of β-Actin. Fold changes were calculated by normalizing the values to the control samples. Data were analyzed with the GraphPad software or excel and were represented as mean ± SEM. Experimental results significance was evaluated by the Student's t-test. A p-value <0.05 was considered as statistically significant. Statistical details, including n, mean, and SEM, are detailed in the figure legends.